2019 丘成桐中学科学奖

基于步进频信号磁共振原理的定位与能量传输一体化系统研究

姓　　名：刘昱麟（JASON LIU）

地　　区：美国

学　　校：威奇托市独立学院

指导老师：Jim Harris

Integration of Positioning and Energy Transmission with Stepped Frequency Chirp Signal Magnetic Resonance

YuLin Liu
The Independent School
Wichita, 67207, Kansas, USA
jason.liu@theindependentschool.com

***Abstract*—An integration scheme for high-precision remote positioning and energy transmission with step-frequency-signal magnetic resonance is proposed. A stepped frequency chirp signal (SFCS) is employed as the driving signal to track the optimal resonant frequency that will maximize the transmission power of two resonant coils, leading to high-precision remote ranging due to the highest signal-to-noise ratio at the receiving coil. This scheme is very useful in unmanned factory where ranging information for positioning and energy transmission for charging are required by unmanned vehicles. Compared with the method coupled without resonance, the ranging accuracy is increased by a factor of four in the same ranging scope, or the ranging scope is increased by an order of magnitude with the same ranging accuracy. Also, the ranging accuracy is increased by 5dB and about 50% gain of energy transmission efficiency could be obtained compared with the step frequency scheme.**

***Keywords*—magnetic resonance, stepped frequency chirp signal, SFCS, ranging, positioning, energy transmission**

I. Introduction

In recent years, major economies around the world have been vigorously promoting the revival of manufacturing. Under the enthusiasm of Industry 4.0, Industrial Internet, Internet of Things, and cloud computing, many excellent manufacturing companies around the world have developed smart factory construction practices [1]. For example, Siemens Amberg Electronics Factory has realized the mixed production of multi-variety industrial computer; FANUC has realized the high degree of automation and intelligence of the robot and servo motor production process, and utilizes the intelligent warehouse of various intelligent manufacturing units in the workshop. Transferring materials to achieve unattended maximum 720 hours; Harley-Davidson Company of the United States makes extensive use of intelligent manufacturing units consisting of machining centers and robots to achieve mass customization; Mitsubishi Electric Nagoya Manufacturing Co., Ltd. adopts a new robot assembly line that combines man and machine. The transformation from automation to intelligence has significantly increased the production per unit of production area; the global heavy truck giant MAN has built a complete in-plant logistics system, using AGV to load the assembled components and the whole vehicle, which is convenient for flexible adjustment of the assembly line. A material supermarket was established and achieved remarkable results. The smart robot is the key role to make the the factory to work well. Therefore, a large-scale, and accurate positioning technology is demanded to ensure the robot work well in the factory.

However, traditional positioning methods like optical based positioning method will suffer from problem of the sight occlusion, inertial navigation based positioning method has problem of measure drifting and the electromagnetic wave positioning method will lose the positioning accuracy because of multi-path [2]. Compared to these traditional positioning methods, the magnetic positioning methods not only don't have these problem, but also can achieve the millimeter positioning accuracy. Magnetic positioning is a method of obtaining the position and spatial attitude of an object using a magnetic field. It has been widely used in aiming, motion tracking, free arm three-dimensional ultrasound imaging and many other fields. Compared with other spatial positioning methods, magnetic positioning has the advantages of no damage, no line of sight, easy operation. The earliest traditional methods based on magnetic coupling proposed by 1975 J. Kuipers [3] and the method proposed by F. H. Raab in 1977 [4]. However, the positioning range is severely restricted because of the amplitude of the magnetic field decays by 3 times with distance. In 2007, the Marin Soljacic group at the Massachusetts Institute of Technology published a paper on high-efficiency energy transmission based on magnetic field resonance. In this paper, magnetic field resonance was used to successfully illuminate a 60 W bulb outside 2 m with a transmission efficiency of 40 [5]. The principle is that when the transmitting coil and the receiving coil have the same resonant frequency, the impedance between the two coils is minimized and the energy transmission efficiency is maximized under the driving of the resonant frequency. Since then, the power transfer, magnetic positioning and magnetic communication based on magnetic resonance have become a research hotspot. A magnetic resonance localization method based on the magnetic dipole model is proposed by Ref. [6]. Establishing the reflection coefficient between the coupled coils and the coordinate positions of the two coils, the geometric positioning method is adopted. Complete positioning of the target coil. At a distance of 1.686 m, the average positioning error is 0.61 cm. Dionigi proposed a method by using a high-Q resonant circuit, which can improve the accuracy of ranging based on

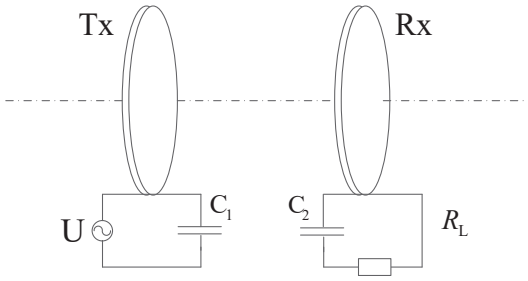

Fig. 1. General schematic diagram of two coupled magnetic resonance coils

magnetic resonance method, but it can not guarantee that the transmission power is kept at the maximum value in real time, so the accuracy improvement is restricted [7]. The Ref. [8] proposed a Q-controllable resonant circuit to extend the distance of magnetic positioning. However, the design needs to add additional boost coils to compensate the energy in real time. Therefore, the designed system is also complicated and not applicable. For miniaturization. A gesture recognition method based on magnetic resonance localization, which uses multiple transmitting coils to transmit magnetic signals and multiple receiving coils for receiving is also proposed by Ref. [9]. General schematic diagram of two coupled magnetic resonance coils show in Fig. 1. C1 and C2 represent the capacitance of transmitter (Tx) and receiver (Rx), respectively. R_L represents the load resistance which is connected to the Rx. U denotes the source of signal.

Besides the focus on high-performance positioning methods, the power transmission is also conducted researched in this paper. The efficiency will be significantly improved if the robot can not only complete the high precision positioning, but also automatic charging. In order to make the smart factory become more smart. Integration of positioning and energy transmission with stepped frequency chirp signal magnetic resonance has been proposed in this paper. The rest of this paper is summarized as follow: Section II introduces system architecture; Section IV puts up the positioning methods based on chirp-frequency-signal; Section III introduces the proposed energy transmission method. Integration of positioning and energy transmission is introduce in section IV-B3. Section V shows the experimental system and conclusion is explained in the section VI.

II. Ranging and Positioning Method

A. Magnetic resonance method

A resonant system consists of two or more objects with the same Eigen frequency. When resonance occurs between these objects, energy is efficiently transmitted between them, and energy transfer occurs only between these resonant objects, without energy exchange with surrounding objects. The energy transmission efficiency is maximized when resonance occurs, that is, the amplitude of the signal is also maximized. The magnetic resonance system can be analyzed by coupled model theory [5]. For a resonant system composed of two objects, an equation can be established as follows:

$$\begin{cases} \dfrac{\mathrm{d}a_1}{\mathrm{d}t} = -i(\omega_1 - i\gamma_1)a_1 + ika_2 \\ \dfrac{\mathrm{d}a_2}{\mathrm{d}t} = -i(\omega_2 - i\gamma_2)a_2 + ika_1 \end{cases} \tag{1}$$

where $a_1(t)$, $a_2(t)$ denote the amplitude, respectively. Their square of the amplitude represents the energy of the object. ω_1 and ω_2 denotes the eigenfrequencies of two objects, respectively; γ_1, γ_1 denote the intrinsic loss rate of two objects, characterized by energy loss. k denotes the mutual coupling coefficient between two objects. Expressing the formula in a matrix can be written as

$$\begin{cases} \dfrac{\mathrm{d}\mathbf{a}}{\mathrm{d}t} = -i\mathbf{A}\mathbf{a} \\ \mathbf{a} = \begin{bmatrix} a_1 \\ a_2 \end{bmatrix}, \mathbf{A} = \begin{bmatrix} \omega_1 - i\gamma_1 - k \\ -k\omega_2 - i\gamma_2 \end{bmatrix} \end{cases} \tag{2}$$

Since the resonant objects have the same resonant frequency, it can be considered that the conditions are met:

$$\omega_1 = \omega_2 = \omega_0, \gamma_1 = \gamma_2 = \gamma \tag{3}$$

Furthermore, the eigenvalues of the matrix A can be obtained:

$$\omega = \omega_0 - i\gamma \pm k \tag{4}$$

Substitute $e^{j\omega t}$, Assume the time $t = 0$, $a_1(0) = B$, $a_2(0) = 0$, the loss can be ignored when the $k \gg \Gamma$, the equation can be written as:

$$\begin{aligned} \omega_1(t) &= B^2\cos^2(kt) \\ \omega_2(t) &= B^2\sin^2(kt) \end{aligned} \tag{5}$$

$\omega_1(t)$ and $\omega_2(t)$ represent the energy of object 1 and object 2, respectively. According to above the equations, the energy can be transmitted from object 1 to object2 with great efficiency when the $t = \pi/2k$. The coupled parameter k represents the speed of energy transfer.

B. General Positioning method

*1) **WIFI positioning**:* There are two kinds of Wi-Fi positioning technology. One is the wireless signal strength of the mobile device and the three wireless network access points, and the differential algorithm is used to accurately locate the person and the vehicle. The other is to record a huge amount of signal strength at a certain location point in advance, and determine the location by comparing the database with the huge amount of data with the signal strength of the newly added device. Wi-Fi positioning can realize complex large-scale positioning, monitoring and tracking tasks in a wide range of applications. The total accuracy is relatively high, but the accuracy for indoor positioning can only reach about 2m, and it is impossible to accurately locate. Due to the popularity of Wi-Fi routers and mobile terminals, the positioning system can share the network with other customers, the hardware cost is very low, and the Wi-Fi positioning system can reduce the possibility of radio frequency (RF) interference. The fig.xx shows one of the positioning method using Wi-Fi [10].

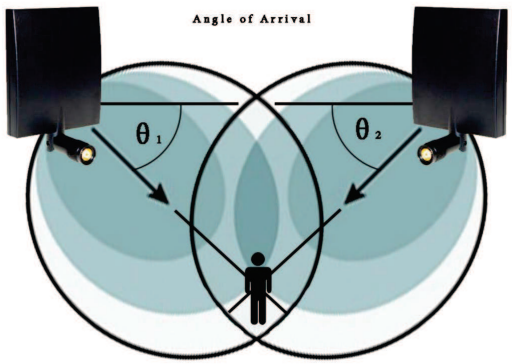

Fig. 2. A special directional Wifi antenna determine the position with Angle of Arrival.

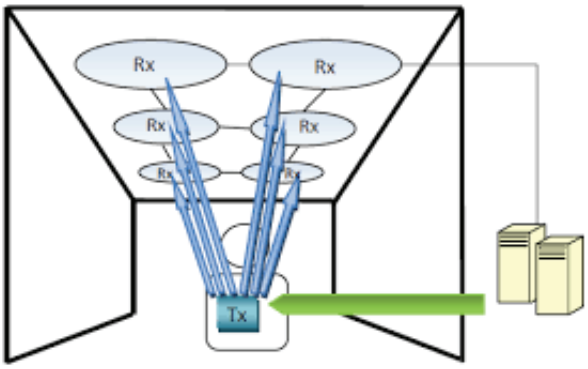

Fig. 3. Active Bat system using ultrasonic positioning method

Fig. 4. Active badges

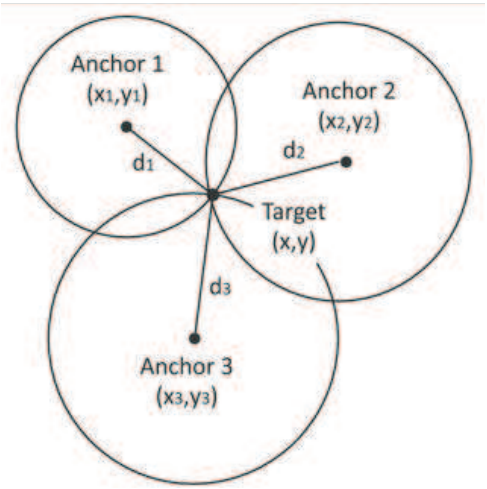

Fig. 5. the principle of the base station positioning method

*2) **Ultrasonic positioning**:* Ultrasonic positioning technology emits ultrasonic signals that can be detected by the terminal microphone by installing a plurality of ultrasonic speakers indoors. The position of the terminal is estimated by the difference in arrival times of different sound waves. Since the transmission speed of sound waves is much lower than that of electromagnetic waves, the system implementation is very difficult, and the wireless synchronization of the system can be realized very simply, and then transmitted by the ultrasonic transmitter, and the receiving end receives the microphone, and the operation position can be performed by itself. Since the rate of sound waves is relatively low, it takes a long time to transmit the same content, and only a TDoA-like way can obtain a larger system capacity [11]. The active bat system using ultrasonic positioning method shown in Fig. 3.

*3) **Infrared positioning**:* The principle of infrared indoor positioning technology positioning is that the infrared ray emits modulated infrared rays and is received by an optical sensor installed indoors for positioning. Although infrared rays have relatively high indoor positioning accuracy, infrared rays can only be transmitted by line of sight because light cannot pass through obstacles. The two main disadvantages of linear line of sight and short transmission distance make the indoor positioning effect very poor. When the logo is placed in a pocket or has walls and other obstructions, it will not work properly. It is necessary to install a receiving antenna in each room and corridor, which is expensive. Therefore, infrared rays are only suitable for short-distance propagation, and are easily interfered by fluorescent lamps or lights in a room, and have limitations in precise positioning. Active badges (shown in Fig. 3) is the first indoor location sensing system developed by AT&T Cambridge using infrared positioning method [12].

*4) **The base station positioning**:* The base station location is generally applied to mobile phone users. The mobile phone base station location service is also called Location Based Service (LBS), which acquires the location information of the mobile terminal user (latitude and longitude coordinates) through the network of the telecommunication mobile operator (such as the GSM network).), with the support of the electronic map platform, a value-added service that provides users with corresponding services, such as the dynamic location query service provided by China Mobile's M-Zone. Since GPS positioning is relatively expensive, base station positioning is a common function of GPS devices. However, the positioning accuracy of the base station is low, generally ranging from 500 meters to 2000 meters [13]. The principle of the base station positioning method shown in Fig. 4.

III. Energy Transmission Method

A. General energy transmission method

1) Electromagnetic radio-energy transmission: Electromagnetic radiation radio energy transmission is a long distance

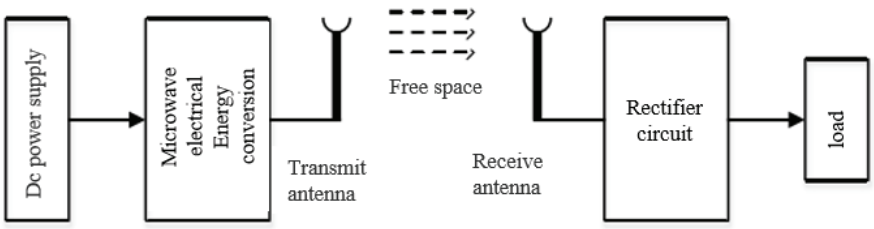

(a) Electromagnetic radio-energy transmission.

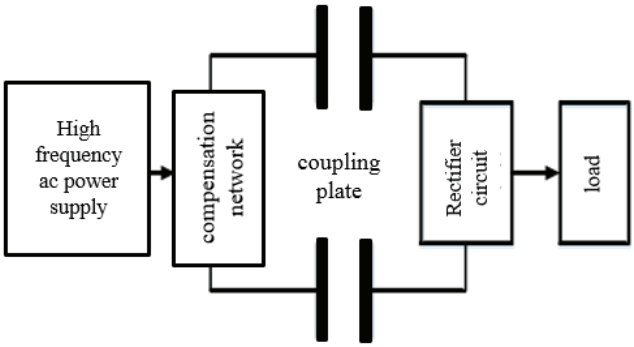

(b) Electric field-induced radio energy transmission.

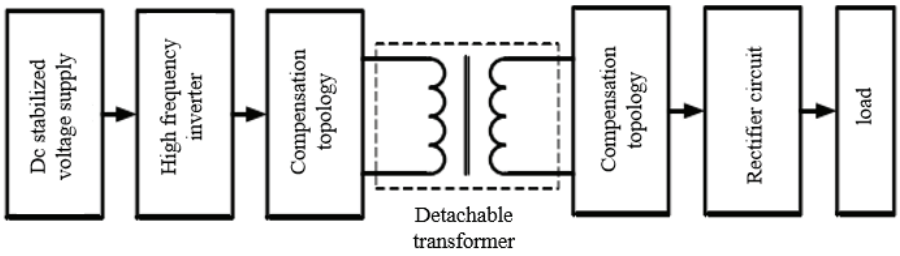

(c) Magnetic induction coupled radio energy transmission.

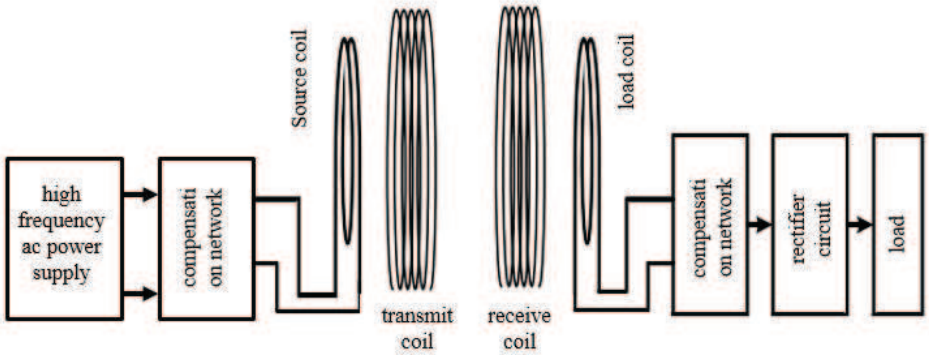

(d) Magnetically coupled resonant radio energy transmission.

Fig. 6. General energy transmission method.

wireless transmission mode, including microwave electromagnetic radiation radio transmission and laser electromagnetic radiation radio transmission two ways [14]. Microwave radiometer can radio transmission as shown in Fig. 6(a). The basic principle of electricity-microwave switching device to convert dc to microwave energy, the transmitting antenna to microwave energy emitted electromagnetic beam after a long distance of free space to receiving antenna is collected, then through microwave rectification device into direct current, then for the use of the load.

2) Electric field-induced radio energy transmission: Wireless energy transmission based on electric field induction coupling, also known as capacitive wireless energy transmission, realizes the wireless energy transmission through the coupling capacitance between the plates [15]. The electric field induction radio energy transmission system is composed of three modules: transmitting circuit, coupling electrode plate and receiving circuit. The transmitting circuit includes high-frequency ac power supply and compensation network circuit, and the receiving circuit includes rectifying and filtering circuit and load. As shown in Fig. 6(b), the electric field-induced radio energy transmission system is powered by high-frequency ac power supply. The transmitting end of the coupling plate is connected with the high-frequency ac power supply. The coupling plate generates an electric field under the excitation of alternating current, thus generating displacement current at the receiving end of the coupling plate. The displacement current feeds the load after passing through the rectified filter circuit. The compensation inductance can reduce the reactive power output of the high frequency inverter, and the resonance can increase the voltage between the coupling plates. The coupling plate is the core part of the system, which uses the changing electric field to realize the power transfer from the primary side to the secondary side.

3) Magnetic induction coupled radio energy transmission: Magnetic induction coupled radio energy transmission technology puts the primary coil and secondary coil on adjacent positions. When high-frequency alternating current passes through the primary coil, according to the principle of electromagnetic induction, induced electromotive force is generated in the secondary coil, so as to realize non-contact transmission of electric energy [16]. Magnetic induction coupled radio energy transmission mainly includes two structural forms, one is the separable transformer type with iron core [17], and the other is the hollow coil pure induction type without iron core [18]. The schematic diagram of magnetic induction coupling radio energy transmission system based on separable transformer is shown in Fig. 6(c), which mainly includes DC voltage stabilizing power supply, high-frequency inverter, primary side compensation topology, separable transformer, secondary side compensation topology and rectifier voltage stabilizing circuit composition [19], [20]. The high frequency ac current generated by the dc voltage stabilizing power supply is input to the primary side of the separable transformer through the high frequency inverter. Under the effect of the induction coupling of the high frequency electromagnetic field, the electric energy is transmitted to the secondary side, and then the high frequency ac current coupled to the secondary side is converted into direct current for use through the rectifier voltage stabilizing circuit.

4) Magnetically coupled resonant radio energy transmission: Magnetic coupling resonant radio energy transmission technology and magnetic induction coupling radio energy transmission technology are the same use of electromagnetic energy conversion near the field to achieve the wireless transmission of energy, but on this basis, magnetic coupling resonant radio energy transmission technology USES the resonance technology of transmitter and receiver [21].

Magnetically coupled resonant radio energy transmission system is shown in Fig. 6(d), which is mainly composed of high-frequency ac power supply, source coil compensation network, resonant coil and load coil, load coil compensation network and rectifier voltage regulator circuit, etc. The resonant coil is composed of transmitting coil and receiving coil, both of which have the same resonant frequency. The working principle of magnetic coupling resonant is that high frequency alternating magnetic field is produced when high frequency ac power source going through the coil, and this is transmitted to the receiving coil. Since the same resonance frequency is shared between the receiver and the transmitter coil, magnetic resonance occurs, and the transmitter coil energy can transfer to the load coil. Achieving a high efficient energy transmission from the transmitter to the receiver [22][23]. Compared with magnetic induction coupled radio energy transmission, magnetic coupled resonant radio energy transmission USES resonance principle to realize the wireless transmission of electric energy in the medium distance and improve the transmission efficiency of electric energy. In addition, the wireless transmission of energy is realized through coil resonance. Only with the same resonant frequency can the object generate energy conversion, so the generated magnetic field will not be affected by non-magnetic media [24], which has a good prospect in the wireless charging application of implantable medical devices. In addition, magnetic coupling resonant radio energy transmission technology used in mouse, mobile phone, remote control and other small power portable equipment greatly reduces the use of batteries, is conducive to environmental protection, has a high research value.

IV. System Architecture

When the distance between the transmitter and receiver is changing, the signal-to-noise ratio (SNR) of the receiver cannot always be kept at the highest level with the transmitting coil excited by the single frequency signal. This is because the optimal resonant frequency maximizing the transmission power of two resonant coils varies with the distance between two resonant coils [25]. Though, resonance frequency of the adaptive tracking control strategy proposed by literature [26], an additional radio frequency (RF) communication module needed to be added to the system. The load power sampled by the receiver state detection module is sent to the receiver in real time to maintain the resonance running state combined with the optimal control algorithm, dynamic adjustment system driving signal frequency. The method for solving problem caused by actual working parameter deviating from the optimal operation parameters is practical and effective, but RF

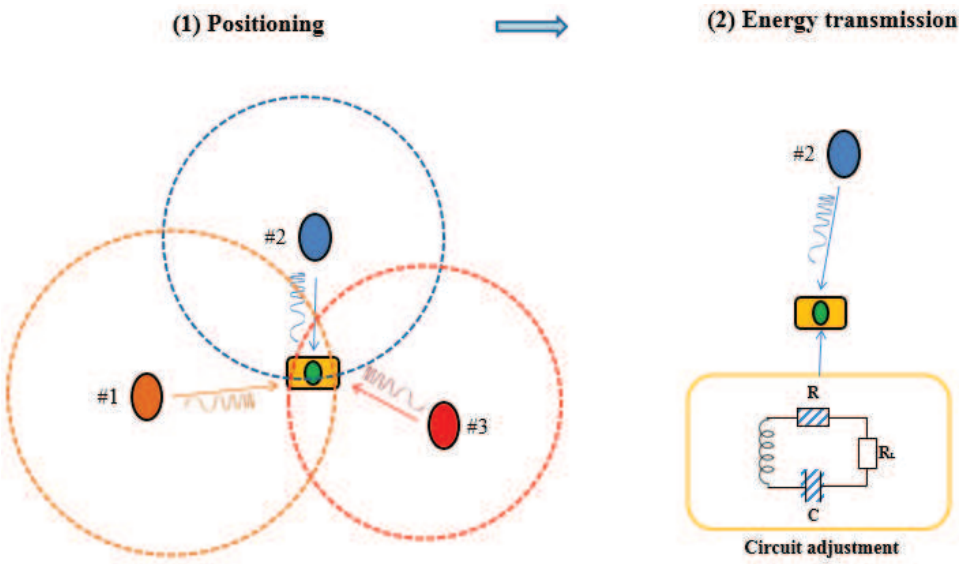

Fig. 7. System structure of integration scheme.

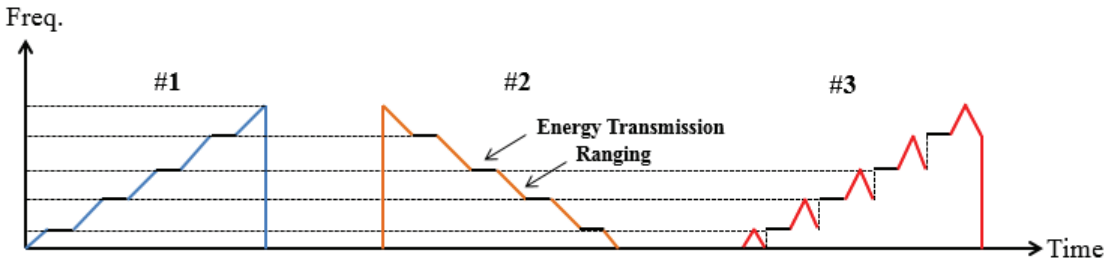

Fig. 8. Realtime magnetic resonance energy transmission.

communication module need to be added, resulting in a system with large volume, complicated structure.

In this context, a stepped frequency chirp signal (SFCS) is proposed in this paper as the driving signal to track the optimal resonant frequency that will maximize the transmission power of two resonant coils. Furthermore, based on this idea, a method for integration of positioning and energy transmission is elaborately designed which would be a promising scheme in the unmanned factory.

The system architecture is illustrated in Fig. 7. Three coils are used for positioning. All of them are excited by SFCS with different chirp slopes which are used for identification as shown in Fig. 8. These kinds of chirp patterns can be implemented by lookup table at the transmitter. By calculating the real-time coupling frequency, the slope pattern with STFT is obtained. Therefore, the corresponding coil could be identified. Since chirp signals are used, a large scope of continuous frequency can be obtained, making it possible to achieve the real optimal resonance. In this context, the maximum signal-to-noise (SNR) is obtained because of the maximum resonant amplitude of the receiving coil, resulting in highest ranging accuracy. Moreover, as long as the distances between the receiving coil and the transmitting coils are calculated, the location of the receiving coil is obtained by geometric positioning method. Moreover, the periodic silence between the chirp patterns can be used for time synchronization at the receiver. This timing information would be used for energy transmission.

Since the circuit parameters of the transmitters are unknown to the receiver, as long as the positioning information is obtained, the energy transmission can be implemented by adjusting the circuit parameters to track the optimal resonant frequency.

A. Magnetic Ranging method

1) Step-frequency-signal magnetic ranging method: A high positioning precision method using magnetic ranging based on step frequency signal driven is proposed by Ref.[27]. Firstly. According to the reference, the optimal resonant frequency, which maximizing the load voltage, will vary with the distance between Tx and Rx. The equation can be expressed as follows:

$$U = \frac{\omega M^2 V_i R_{\mathrm{L}} (2R_{\mathrm{L}} Z_0 + R_{\mathrm{L}}\sqrt{\omega} K_1 + Z_0\sqrt{\omega} K_2 - 2\omega^2 M^2)}{(Z_0 R_{\mathrm{L}} + \omega K_1 K_2 + R_{\mathrm{L}} K_1\sqrt{\omega} + Z_0 K_2\sqrt{\omega} + \omega^2 M^2)^3} \tag{6}$$

where K_{12} is a constant term, Z_0 is equivalent resistance and also a constant term. M denotes the mutual coupling coefficient between TX and RX. V_i is voltage of the source. And the load voltage will get the maximum when the frequency of signal satisfies the equation

$$2R_{\mathrm{L}} Z_0 + R_{\mathrm{L}}\sqrt{\omega} K_1 + Z_0\sqrt{\omega} K_2 - 2\omega^2 M^2 = 0. \tag{7}$$

The distance can be got form the mutual coupling coefficient (M) after the maximum of load voltage is obtained. The distance d between Tx and Rx can be expressed as:

$$d = (\frac{\mu\pi N_{\mathrm{t}} N_{\mathrm{r}} a_{\mathrm{t}}^2 a_{\mathrm{r}}^2}{2M})^{1/3}. \tag{8}$$

where $\mu, \mathrm{N}_t, a_t, \mathrm{N}_r, a_r, M, \mathrm{d}$ denote the magnetic medium constant, the turns number of the TX coils, the radius of the TX coil, the turns number of RX coil, the radius of the RX coil, mutual coupling coefficient and the distance of the TX coil and RX coil, respectively. Thus, it plays a key role in tracking the optimal resonant frequency in real time when the distance between Tx and Rx varying. Under optimal resonant frequency, the ranging scope can be extended. subsubsectionStep-frequency chirp signal magnetic ranging method

*2) **Ranging with Stepped Frequency Chirp Signal**:* According to the Ref. [27], the optimal resonant frequency, which maximizing the load voltage, will vary with the distance between Tx and Rx. Thus, it plays a key role in tracking the optimal resonant frequency in real time when the distance between Tx and Rx varying. Under optimal resonant frequency, the ranging scope can be extended. Here, compared with Ref. [27] where stepped frequency is used for driving, to further refining the resonant frequency, giving larger resonance amplitude, a stepped frequency chirp signal (SFCS) to proposed to drive the Tx coil. The SFCS is expressed as

$$\begin{aligned} s(t) &= \frac{1}{\sqrt{NT}} \sum_{t=0}^{N-1} u(t - iT_r) \exp(j2\pi f_i t) \\ &= \frac{1}{\sqrt{NT}} \sum_{t=0}^{N-1} \mathrm{rect}\left(\frac{t - iT_r}{T}\right) \exp\left[j\pi K (t - iT_r)^2\right] \\ &\quad \times \exp\left[j2\pi (f_0 + i\Delta f) t\right] \end{aligned} \tag{9}$$

Where $K = B/T$ is the slope of frequency modulation of Chirp signal, T_r is the pulse repetition period, T is the pulse width, f_0 is the center frequency of the and $u(t) = \mathrm{rect}\left(\frac{t}{T}\right) \exp\left(j\pi K t^2\right)$ is the sub-pulse of the chirp signal, $f_i = f_0 + i\Delta f$ is the carrier frequency of the i-th Chirp sub-pulse. The illustration of frequency-stepped chirp signal is shown in Fig. 9.

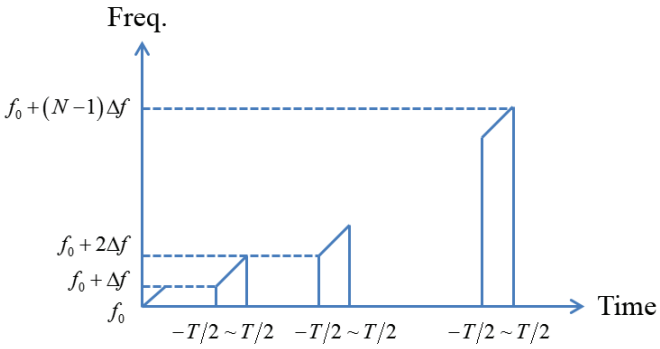

Fig. 9. The relation between frequency and time of SFCS.

*3) **Higher positioning by Kalman filtering**:* Since the positioning result of this method is discrete, the inertial navigation devices such as accelerometer or the gyroscope installed on the vehicle can be used for continuous positioning by Kalman filtering, as illustrated in Fig. 10. In the discrete time instance, such as point $k-1$ and point k, magnetic positioning results are obtained and Kalman filtering used for positioning calibration such its high accuracy. While in the continuous time, such as point 1, point 2, and point 3, only positioning results come from inertial navigation devices can be obtained. In this case, Kalman recursion based on one-step estimation and filtering is employed for continuously positioning. Only in this way, could be positioning accuracy be increased by combing the continuously inertial navigation results and the discrete magnetic positioning.

B. Energy transmission

1) Electromagnetic induction mode: This charging method is realized by passing the current through the coil, and the coil generates magnetic field and generates induced electromotive force to the nearby coil, thus generating current. This charging method has a high conversion efficiency, but the transmission distance is short, reaching about 0 mm $\sim$ 10 cm, and it requires a higher position. So it can only be carried out one-to-one with the coil. Metal induction contact will also generate heat resulting in heat. Wireless charging technology based on magnetic field induction is essentially similar to hollow transformer, with simple principle, mature technology and low cost. It is a widely used technology. However, the disadvantages of magnetic induction technology are short transmission distance and low degree of freedom of placement of charging devices.

2) Magnetic resonance mode: Charging with magnetic resonance is first proposed by MIT in 2007, where an electric bulb at 2m distance far from the source is illuminated with efficiency of $40\% \sim 50\%$. Compared with other charging technology, magnetic resonance technology can enlarge the charging distance from millimeter to meters, giving high degree for application, such as location detection in industrial, wireless sensor networks, aerospace, implanted artificial

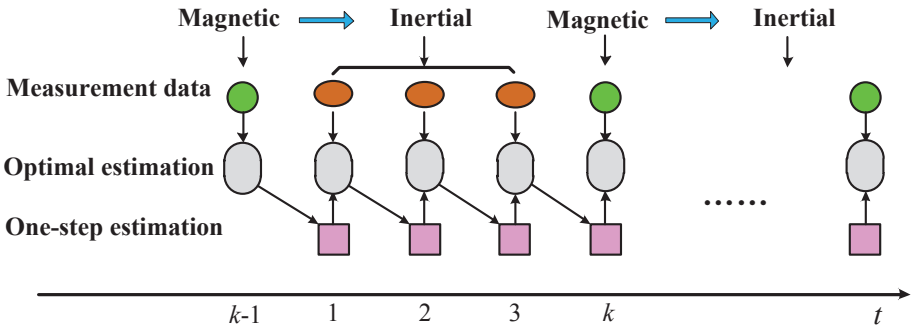

Fig. 10. Processing of Kalman filtering.

organs. Moreover, it is more reliable and can charging with more devices at one time.

The sending end encounters the receiving end with the same resonance frequency, and the power transmission is carried out by the resonance effect. This kind of charging method has long transmission distance and large transmission power, which is suitable for long-distance high power charging. However, this charging method has low efficiency and great loss in the transmission process. The farther the distance, the greater the transmission power and the greater the loss. More importantly, the frequency spectrum used must be protected from outside interference.

In terms of current technologies, both charging methods have certain advantages and disadvantages. Generally speaking, they can only be charged in a fixed position and range, which is not convenient enough for mobile devices. So researchers are trying to develop ways for charging anywhere, anytime.

*3) **Realtime resonance energy transmission**:* As for energy transmission, efficiency of transmission is the key point. If energy transmission could be always implemented at the optimal resonant point, the efficiency can be very high. To this end, an energy transmission scheme based on positioning is elaborately designed as illustrated in Fig. 11.

The procedure of energy transmission can be described as follows:

1) Step 1, positioning is implemented by the fusion of magnetics and inertial devices installed on the vehicle.
2) Step 2, the nearest transmitting coil is selected based on the positioning information, and optimal resonant frequency between these two coils could be calculated.
3) Step 3, since the chirp pattern of the corresponding transmitter is known to the receiver, the circuit parameters of the receiving coil, i.e., resistance and capacitance can be adjusted according to the optimal resonant frequency and the transmitting chirp pattern. Therefore, energy transmission can be performed.

Since the optimal resonance frequency point can be obtained by employing stepped-frequency chirp signal, the energy transmission efficiency can be obtained high compared with other transmission schemes. This can be shown in Fig. 12. For traditional transmission scheme, signal with constant frequency is used, this corresponding to a fixed transmission distance, thus when the receiver moving away from this optimal distance point, the energy transmission efficiency could be decreased. While, when employing stepped-frequency, almost the optimal resonance frequency can be achieved, but still sometimes not the real optimal frequency due to the fact that there is a gap between the real resonance frequency and the observed one which is caused by "frequency step". Fortunately, this can be improved by using chirp signal, where continuous frequency can be obtained. This can result in optimal resonance frequency in realtime. Though the energy transmission efficiency is also not 100%, this is loss caused by the system hardware.

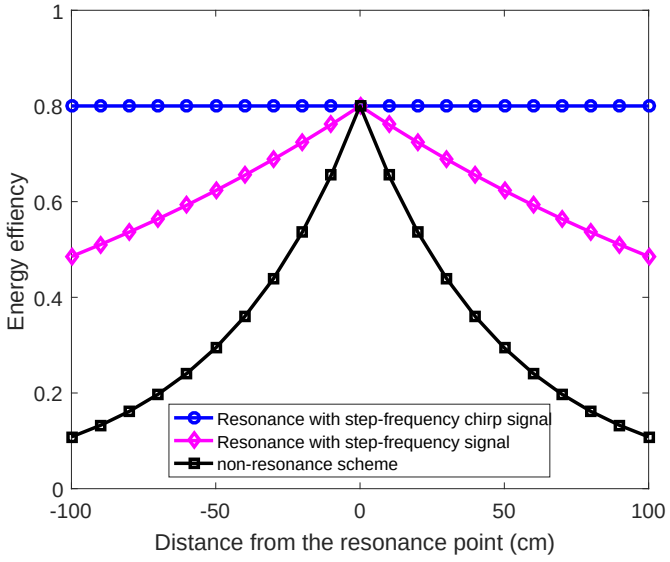

Fig. 12. Energy efficiency.

V. System Verification

A. Theoretical simulation

The transmitting and the receiving coil are with the same parameters shown in Table I. The measured distances of the ranging system with magnetic resonance is simulated.

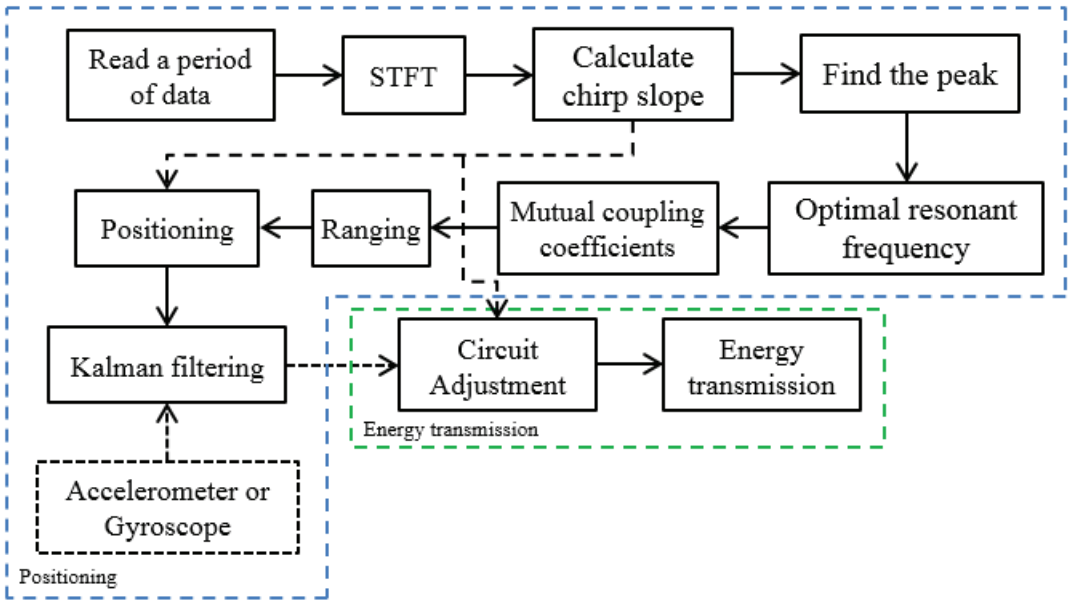

Fig. 11. Processing flow of integration scheme.

TABLE I
SIMULATION PARAMETERS.

Parameters	Value	Dimension
Coil radius r	0.15	m
Coil turns n	18	3
Coil induction L	25.4	μH
Series capacitance C	9.6	nF
Load resistance R	5	Ω
Signal bandwith B	25	MHZ

The root-mean-square error (RMSE) is also calculated to characterize the simulation result. The calculate procedures is same as the Ref. (7) and the formula is

$$\sigma = (\mathrm{m}^{-1} \sum_{i=1}^{m} (x_i - \bar{x})^2)^{\frac{1}{2}} \tag{10}$$

Where x_i is the calculate results and the $\bar{x}$ is the theoretical value.

As shown in the Fig. 13, Compared to the traditional method based on step frequency driving , the ranging precision have been proposed obviously. It is because the optimal resonance frequency cannot always be obtained using the step-frequency-signal to drive the coils. The ranging accuracy is similar when both two method get the optimal resonance frequency. According to above, the proposed method can get the more accuracy voltages in the simulation system so that the ranging accuracy can be improved. Moreover, as is discussed in section IV-A3, with Kalman filtering, the positioning accuracy can be improved as shown in Fig. 14.

B. Experiments

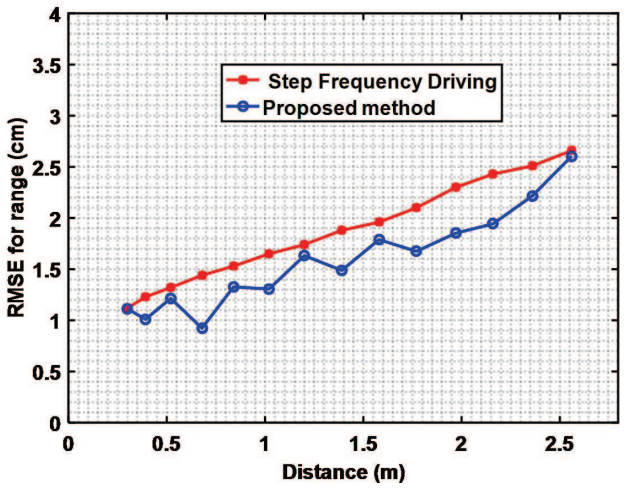

Fig. 13. Ranging accuracy versus distance

1) Hardware System: The basic composition of the positioning and energy transmission system is shown in the Fig. 15, where the light blue arrow indicates that the components are physically connected, and the dark blue arrow indicates that the coil at the transmitting end and the coil at the receiving end are physically isolated in the air. The energy transmission portion includes a charging circuit and a power detecting circuit The core hardware devices include: Three direct digital synthesizers (DDS) are used to generate chirp signals. Three operational amplifiers (OA) are used to amplified the coil coupled signal. Three bandpass filters (BPF) are used to filter the noise in the amplified signal. A Buck step-down charging circuit, a battery protection circuit and a power detection

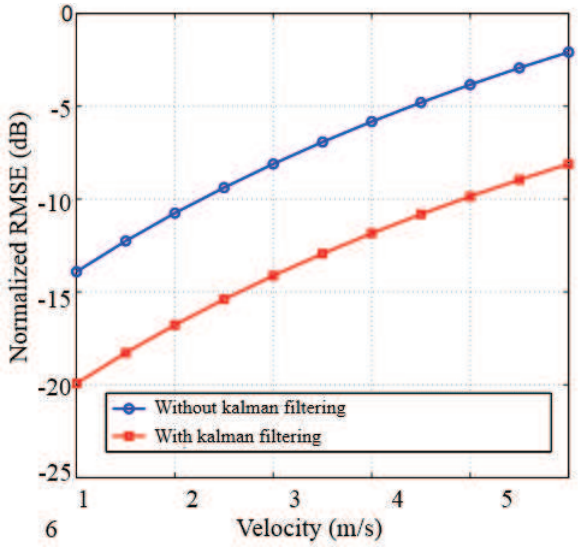

Fig. 14. Positioning accuracy with Kalman data fusion.

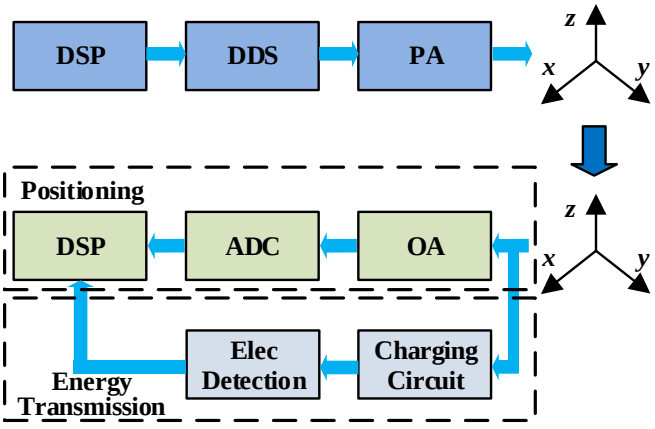

Fig. 15. The basic composition of the positioning and energy transmission system.

circuit for wireless charging. A power amplifier (PA) is used to improve the ability of signal to drive loads. Three Digital-to-analog converters (ADC) are electronic components that converts an analog voltage signal coupled to a sensor into a digital signal. A data operation and control unit (STM32F407VET6) is used to control the system work well and process the signal. Two three-axis coils for coupling the chirp signal and resonant amplification to transmit energy.

I) Power amplifier (TDA7266): The TDA7266 is a bridge amplifier with a maximum output current of 1.5A, a supply voltage of 3 to 18V, and a maximum output power of 10W. In the experimental system, the driving signal is amplified by the power amplifying circuit.

II) ADC (AD7606): The experimental system uses the AD7606 chip of Analog Devices of America as a digital-to-analog converter. The AD7606 is a 16-bit, 8-channel synchronous input channel with a digital-to-analog converter for high-speed synchronous signal acquisition up to 200kHz.

III) Data operation and control unit (STM32F407VET6): The STM32F407VET6 is based on the high-performance ARM Cortex-M4 32-bit RISC core operating at a frequency of up to 168 MHz. The Cortex-M4 core features a Floating point unit (FPU) single precision which supports all ARM singleprecision data-processing instructions and data types. It also implements a full set of DSP instructions and a memory protection unit (MPU) which enhances application security. It incorporates high-speed embedded memories (Flash memory up to 1 Mbyte, up to 192 Kbytes of SRAM), up to 4 Kbytes of backup SRAM, and an extensive range of enhanced I/Os and peripherals connected to two APB buses, three AHB buses and a 32-bit multi-AHB bus matrix.

IV) OA (INA129): A low power general purpose instrumentation amplifier with excellent accuracy. The device is designed with a versatile three-stage operational amplifier and is small enough for a wide range of applications. The current feedback input circuit provides a wide bandwidth even at high gains (200 kHz at $G = 100$).

V) Energy charging (CN3762): It is a PWM buck mode two-cell lithium battery charge management integrated circuit, which independently manages the charging of two lithium batteries. It has the advantages of small package size, few peripheral components and simple use. The CN3762 has turbulent, constant current and constant voltage charging modes, making it ideal for lithium battery charging management. In the constant voltage charging mode, the CN3762 modulates the battery voltage at 8.4V, and can also be adjusted upward through an external resistor; in the constant current charging mode, the charging current is set by an external resistor.

VI) Fuel gauge (DS2438): It is a smart battery monitoring chip, which is a very small, fast and accurate battery detection chip. Temperature measurement, battery voltage detection, battery current measurement, and remaining battery tracking are available on a single bus.

VII) BPF (UAF42): The filter implemented by UAF42 is time-continuous while avoiding switching noise and aliasing errors of switched-capacitor filters. An additional benefit of this state-adjustable topology is that the filter is less affected by external components.

VIII) Power (AMS1117-3.3V TO-252 package): It is a forward low dropout regulator with an output voltage of 3.3V. It is suitable for high efficiency linear regulators. Switching power supply voltage regulator battery charger active small computer system interface terminal notebook computer power management battery powered instrument.

The experimental system is shown in Fig. 16. Of course, the power supply and program download interface named Joint Test Action Group (JTAG) are also included on the board. In addition to the chips on the board, the most common The detail parameters of experimental system shown in components on the board are the peripheral circuitrys of the chips: inductors, capacitors, and resistors. The serial port is used to communicate with the PC software. The coil parameters of the coupled magnetic signal are shown in Table II.

2) Software Design: The software design mainly includes three aspects: the STM32 programming design at the transmitting end, the STM32 programming design at the receiving

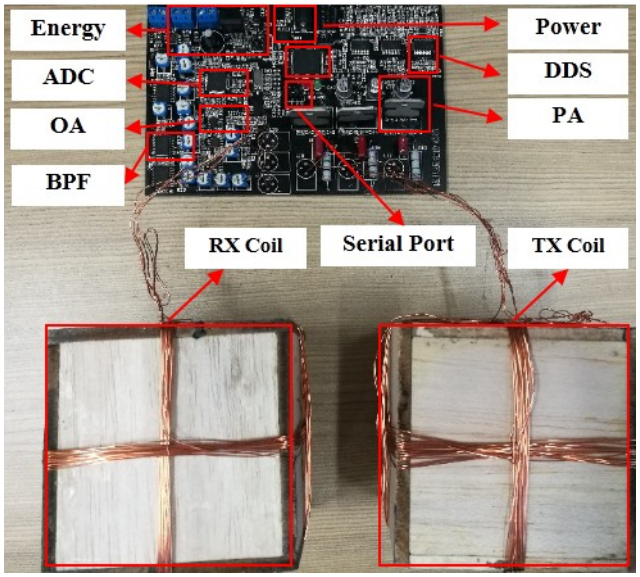

Fig. 16. Experimental system.

TABLE II
EXPERIMENTAL PARAMETERS.

Parameters	Value	Dimension
Coil side length r	0.08	m
Coil turns n	30	3
Coil induction L	10.4	μH
Series capacitance C	7.4	nF
Load resistance R	0.5	Ω
Signal bandwith B	25	MHZ

end and the PC programming design that communicates with the PCB at the receiving end through the serial port within the MODBUS protocol. Besides, STM32 programming belongs to hardware programming using C language, PC programming belongs to upper computer software using C++ language.

I) STM32 programming design at the transmitting end: The programming content of this part is the simplest one. After the STM32 is powered on, it needs to communicate with the DDS, and the hardware SPI mode is used to write the corresponding parameters into the registers of the DDS, and finally the SFCS is generated by setting the signal frequency and phase. Amplification and the RLC resonance of the sinusoidal signal is done by the power amplifier independent of the STM32.

II) STM32 programming design at the receiving end: Compared with the program at the transmitting end, the program at the receiving end is much more complicated, because the algorithm of the entire positioning and energy transmission system runs on the STM32 of the receiving end instead of the transmitting end and the STM32 of the receiving end needs to communicate with the PC host computer. Explain in detail, the program at the transmitting end mainly includes a hardware initialization program, a main control program, a timer interrupt program, and a serial port interrupt program. The program flow chart at the receiving end is shown as the

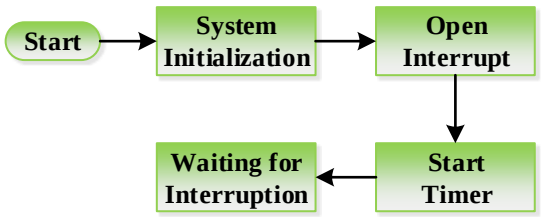

Fig. 17. The program flow chart at the receiving end.

Fig. 17. In the main program, firstly, we initialize the peripherals of the positioning system, including the initialization of the chip AD7606, INA129, UAF42, CN3762, DS2438 and the data memory. Then we start the converter of the AD7606, turn on the ADC, the serial communication interrupt function, the timer interrupt function and set the priority. Finally the master program waits for an interrupt to be triggered. In this system, the A/D sampling rate is 100 kHz, so the sampling time is about 0.01 ms. When the 0:01 ms time arrives, the positioner interrupt is triggered and we read the A/D conversion value. After the timer interrupt operation ends, return to the main program to continue waiting for Interruption. The flow chart of timer interrupt program is shown as Fig. 18. Finally, when the three-axis magnetic field emission of the transmitter is completed in order, the STM32 transmits the A/D data through the serial communication.

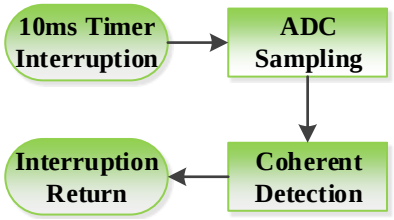

Fig. 18. The program flow chart at the receiving end.

III) PC programming design: The PC program is mainly

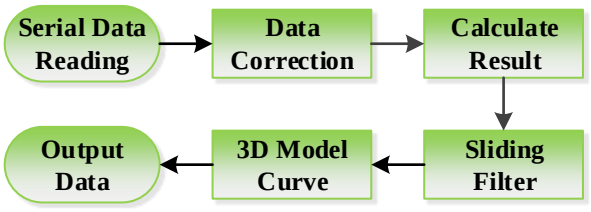

Fig. 19. The data process diagram of PC programming.

responsible for reading data from the serial port, calculating position and attitude, and displaying 3D models. The data process diagram of PC programming is shown in Fig. 19. The data correction unit is used to correct the error caused by the three axes of the sensor which are not being completely orthogonal. Besides, the system error can also be corrected. Firstly, the total distance of the sensor relative to the magnetic source is calculated, then the position coordinates are calculated, and the quadrant is determined. Based on the minimum Euclidean distance discriminant method, the defuzzification operation

is performed. After the position coordinate calculation is completed, the attitude coordinates are solved. Finally, through the sliding filter processing, the curve and the 3D model are drawn, and the position and attitude calculation results are output.

In this positioning and energy transmission system, the interrupt mode design is mainly adopted to improve the program execution efficiency. The lower computer program is written in C language, with clear structure and strong degree of flexibility, which is convenient for debugging and maintenance of the later system. The C++ language is written by the upper computer program. The C++ language is compatible with the advantages of the C language and supports object-oriented programming. The development efficiency is high and the code execution speed is fast. It is suitable for the development of the host computer of this system. The final computer software 3D model display function is as shown in the Fig. 20.

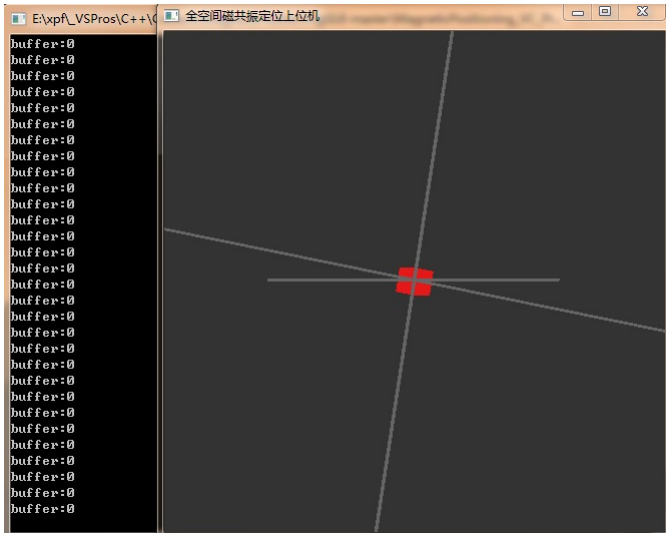

Fig. 20. Computer software 3D model display function.

3) Experimental Results: Experiments can verify the correctness and effectiveness of hardware and software systems. As shown in Fig. 21, after the prepared board is powered up, the SFCS amplified by the power amplifier can be sent, and a slightly distorted sinusoidal signal (noise) can be seen through the oscilloscope at both ends of the receiving coil. As shown in Fig. 22, when the coils at both ends of the transceiver are fixed, a resonance signal can be obtained. When resonance occurs, the amplitude of the signal at the resonance frequency is the largest. The farther from the resonance frequency, the smaller the amplitude of the signal (this is similar to a high Wave packet signal). As shown in Fig. 23, when the STM32 receives the resonant sinusoidal signal and sends it to the host computer software through the serial port through the ADC sampling, the host computer software solves the orientation, distance and attitude of the transmitting three-axis coil from the receiving coil through the positioning algorithm. The energy can be transferred through the Buck circuit and the charging chip (the transmitted energy is stored in the lithium battery).

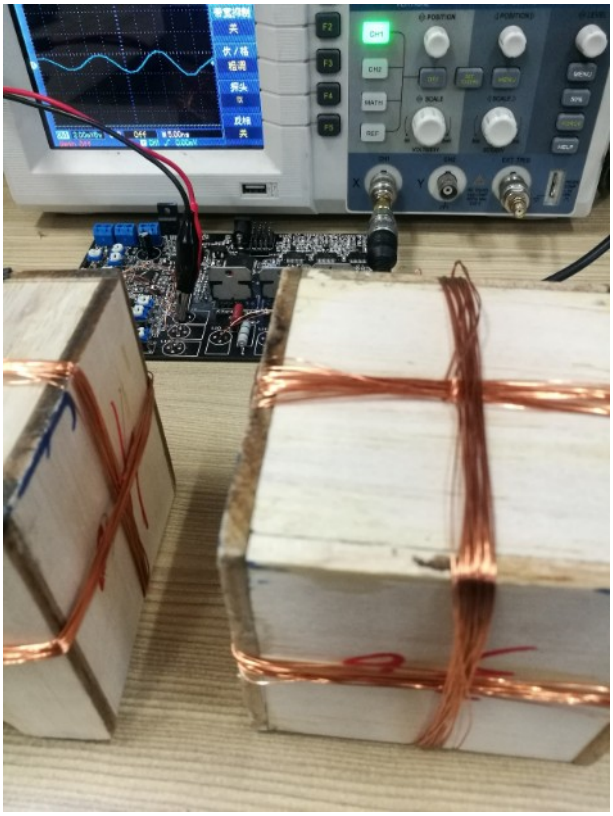

Fig. 21. Receiving a sinusoidal signal received by a three-axis coil.

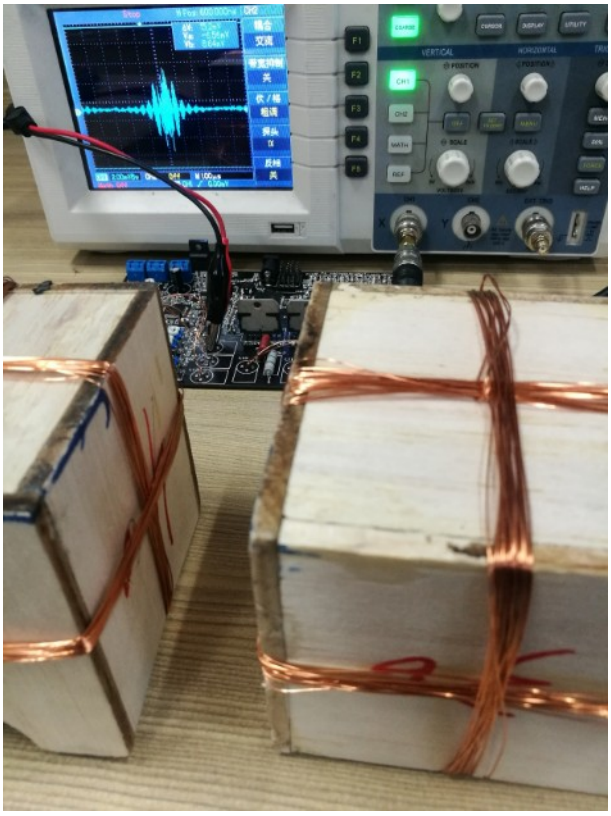

Fig. 22. Resonance signal when the receiving coil and the transmitting coil resonate.

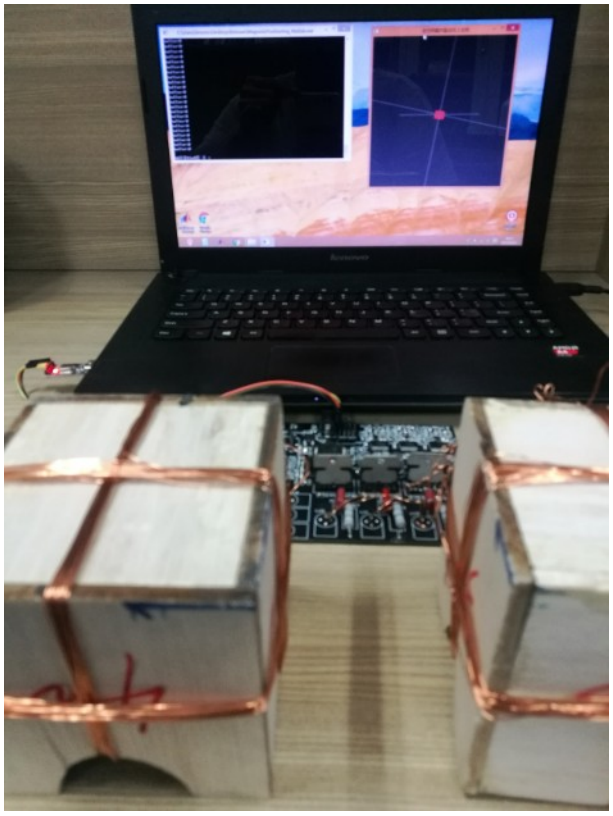

Fig. 23. Joint debugging of hardware system and host computer software.

VI. Conclusion

A stepped frequency chirp signal (SFCS) is employed as the driving signal to track the optimal resonant frequency that would maximize the transmission power of two resonant coils, which can give high-precision remote ranging due to the highest signal-to-noise ratio of the receiving coil. For positioning, three transmitting coils are used for positioning with three different chirp patterns. To further increase the positioning accuracy, a data integrated navigation method by combing the magnetic positioning and inertial navigation with Kalman filtering. Since magnetic resonance can be obtained, an energy transmission scheme is designed with high efficiency. By simulations, the ranging accuracy is increased by 5dB and about 50% gain of energy transmission efficiency could be obtained compared with the step frequency scheme.

References

[1] Sniderman. B, Mahto. Mo, Cotteleer. Mark J. "Industry 4.0 and manufacturing ecosystems Exploring the world of connected enterprises" (PDF). Deloitte. Retrieved 25 June 2019.

[2] Z. Sun and I. F. Akyildiz, "Underground Wireless Communication Using Magnetic Induction," 2009 IEEE International Conference on Communications, Dresden, 2009, pp. 1-5.

[3] Kuipers J. Object tracking and orientation determination means, system and process: US Patent, 3868565. 1975-2-25.

[4] Raab F H. Remote object position locater: US Patent, 4054881. 1977-10-18.

[5] Kurs, A. , et al. "Wireless Power Transfer via Strongly Coupled Magnetic Resonances." Science 317.5834(2007):83-86.

[6] Arumugam D D, Rickettes D S, et al. "Passive magnetoquasistatic position measurement using coupled magnetic resonances". IEEE Antennas and Wireless Propagation Letters. 2013, 12, 539-542.

[7] Dionigi, Marco , and M. Mongiardo. "Magnetically coupled resonant Wireless Power Transmission systems with relay elements." Microwave Workshop Series on Innovative Wireless Power Transmission: Technologies IEEE, 2012.

[8] Nakamura S, Namiki M, Sugimoto Y, et al. Q controllable antenna as a potential means for wide-area sensing and communication in wireless charging via coupled magnetic resonances[J]. IEEE Transactions on Power Electronics, 2017, 32(1):218-232.

[9] Pirkl G, Stockinger K, Kunze K, et al. "Adapting magnetic resonant coupling based relative positioning technology for wearable activity recognition". 12th IEEE International Symposium on Wearable Computers. IEEE, 2018:47-54.

[10] Beom-Ju Shin, Kwang-Won Lee, Sun-Ho Choi, Joo-Yeon Kim, Woo Jin Lee and Hyung Seok Kim, "Indoor WiFi positioning system for Android-based smartphone," 2010 International Conference on Information and Communication Technology Convergence (ICTC), Jeju, 2010, pp. 319-320.

[11] Hakan Koyuncu, Shuang Hua Yang, "A Survey of Indoor Positioning and Object Locating Systems". IJCSNS International Journal of Computer Science and Network Security, VOL.10 No.5, May 2010

[12] R.Want , A.Hopper,V.Falcao and J.Gibbons; The active Badge location system,ACM Transactions on Information systems Vol. 40, No. 1, pp. 91-102, January 1992

[13] M. Borenovic and A. Neskovic, "Base station positioning using statistical averaging of ray intersection points," 2012 20th Telecommunications Forum (TELFOR), Belgrade, 2012, pp. 338-341.

[14] Schuder J, Gold J, Stephenson H. "An Inductively Coupled RF System for the Transmission of 1 kW of Power Trhough the Skin." Biomedical Engineering, IEEE Transsactions on, 1971, 18(4): 265-273.

[15] Yang, Zhi , W. Liu , and E. Basham. "Inductor Modeling in Wireless Links for Implantable Electronics." IEEE Transactions on Magnetics 43.10(2007):3851-3860.

[16] Si, Ping , et al. "A Frequency Control Method for Regulating Wireless Power to Implantable Devices." IEEE Transactions on Biomedical Circuits and Systems 2.1(2008):22-29.

[17] Ahn, Dukju , and S. Hong. "Wireless Power Transmission With Self-Regulated Output Voltage for Biomedical Implant." IEEE Transactions on Industrial Electronics 61.5(2014):2225-2235.

[18] Harada, Koosuke , W. J. Gu , and K. Murata. "Controlled resonant converters with switching frequency fixed." Power Electronics Specialists Conference IEEE, 1987.

[19] Jaegue Shin, Seungyong Shin, Yangsu Kim. "Design and Implementation of Shaped Magnetic-Resonance-Based Wireless Power Transfer System for Roadway-Powered Moving Electric Vehicles." IEEE Transactions on Industrial Electronics 61.3(2014):1179-1192.

[20] Lee, Byunghun, M. Kiani, and M. Ghovanloo. "A Smart Wirelessly Powered Homecage for Long-Term High-Throughput Behavioral Experiments." IEEE Sensors Journal 15.9(2015):4905-4916.

[21] Kurs, A. , et al. "Wireless Power Transfer via Strongly Coupled Magnetic Resonances." Science 317.5834(2007):83-86.

[22] Sample, A. P , D. A. Meyer , and J. R. Smith. "Analysis, Experimental Results, and Range Adaptation of Magnetically Coupled Resonators for Wireless Power Transfer." IEEE Transactions on Industrial Electronics 58.2(2011):544-554.

[23] Huang, Shoudao, et al. "A Comparative Study Between Novel and Conventional Four-Resonator Coil Structures in Wireless Power Transfer." IEEE Transactions on Magnetics 50.11(2014):1-4.

[24] Zhou Hong, Jiang Yan, Hu Wenshan, etc., "Review and Research on Health and Safety Issues for Magnetically-Coupled Resonant Wireless Power Transfer Systems." Transactions of China Electrotechnical Society 31. 2 (2016): 1-9.

[25] A. P. Sample, D. T. Meyer and J. R. Smith, "Analysis, Experimental Results, and Range Adaptation of Magnetically Coupled Resonators for Wireless Power Transfer," in IEEE Transactions on Industrial Electronics, vol. 58, no. 2, pp. 544-554, Feb. 2011.

[26] Kim, Nam Yoon , K. Y. Kim , and C. W. Kim . "Automated frequency tracking system for efficient mid-range magnetic resonance wireless power transfer." Microwave & Optical Technology Letters 54.6(2012): 1423-1426.

[27] Hong WU, Pengfei XU, Xuefeng JIANG, Chao ZHANG.High Precision Remote Ranging Method with Step Frequency Signal Magnetic Resonance[J]. IEEE Magnetics Letters, April 9, 2018.

Appendix

The appendix chapter is divided into two parts. The first part is the design of the hardware circuit. The Altium Designer

software is used to complete the device selection, principle library and PCB library drawing, magnetic resonance positioning schematic and PCB drawing. The second part is the software code design of the lower computer STM32 and the software design of the upper computer. The software frame of the lower computer uses the Arduino framework, and the upper computer uses OpenGL to complete the mapping of the 3D object and the coordinate axis.

A. Hardware Design

The hardware design mainly includes the design of the top layer circuit and the subsystem circuit. The top circuit diagram is shown in Fig. 24, including the transmit signal portion, the receive signal portion, and the energy storage portion. The core of the subsystem circuit diagram is the STM32 microcontroller, and its schematic diagram is shown in Fig. 25. The schematics of the signal generator and ADC are shown in Fig. 26 and Fig. 27, respectively.

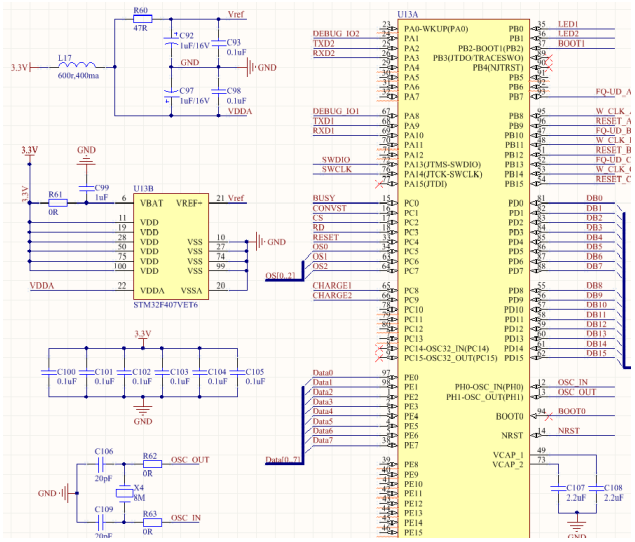

Fig. 25. The subsystem circuit diagram is the STM32 microcontroller.

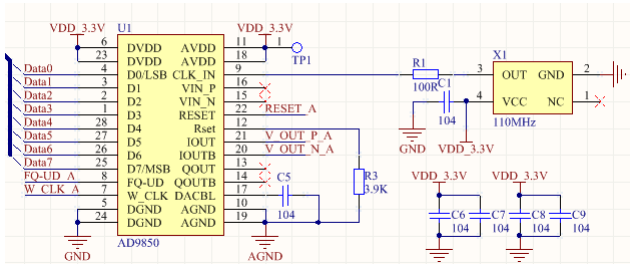

Fig. 26. The schematics of the signal generator.

B. Software Code

The software code of the appendix is also divided into STM32 and PC parts. The engineering structure of the STM32 program with the Arduino framework is shown as Fig. 29. It mainly includes the system library program, the custom library

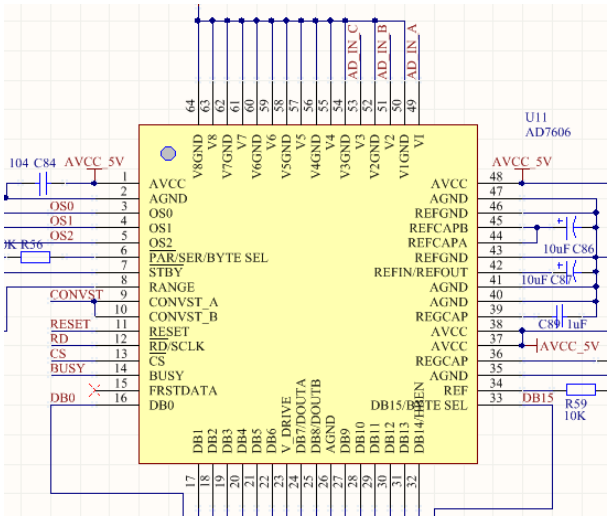

Fig. 27. The schematics of the ADC.

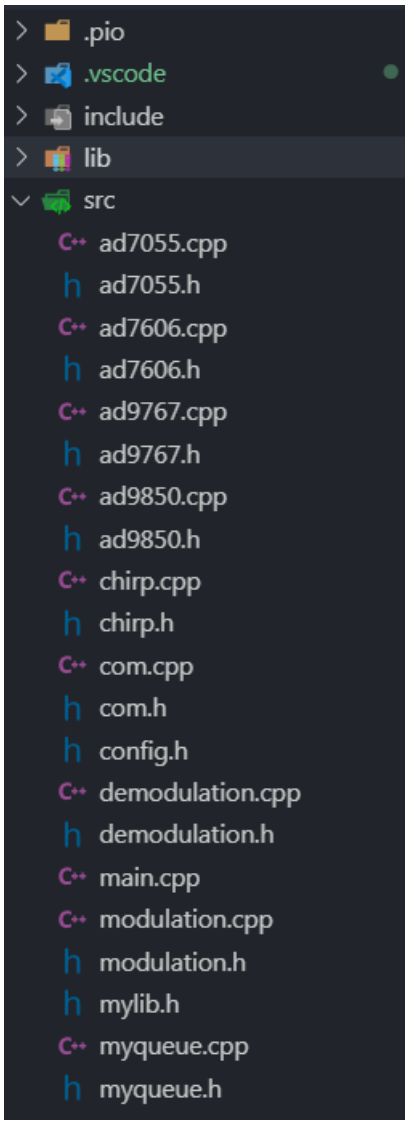

Fig. 29. The engineering structure of the STM32 program.

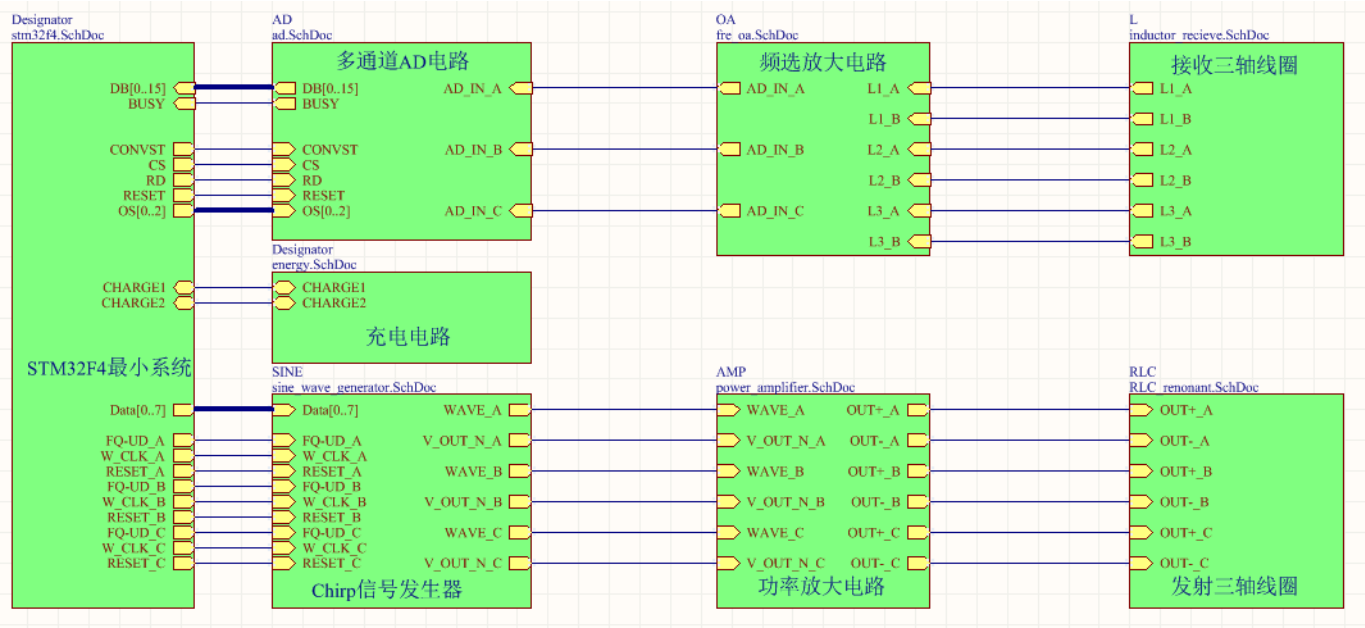

Fig. 24. The top circuit diagram.

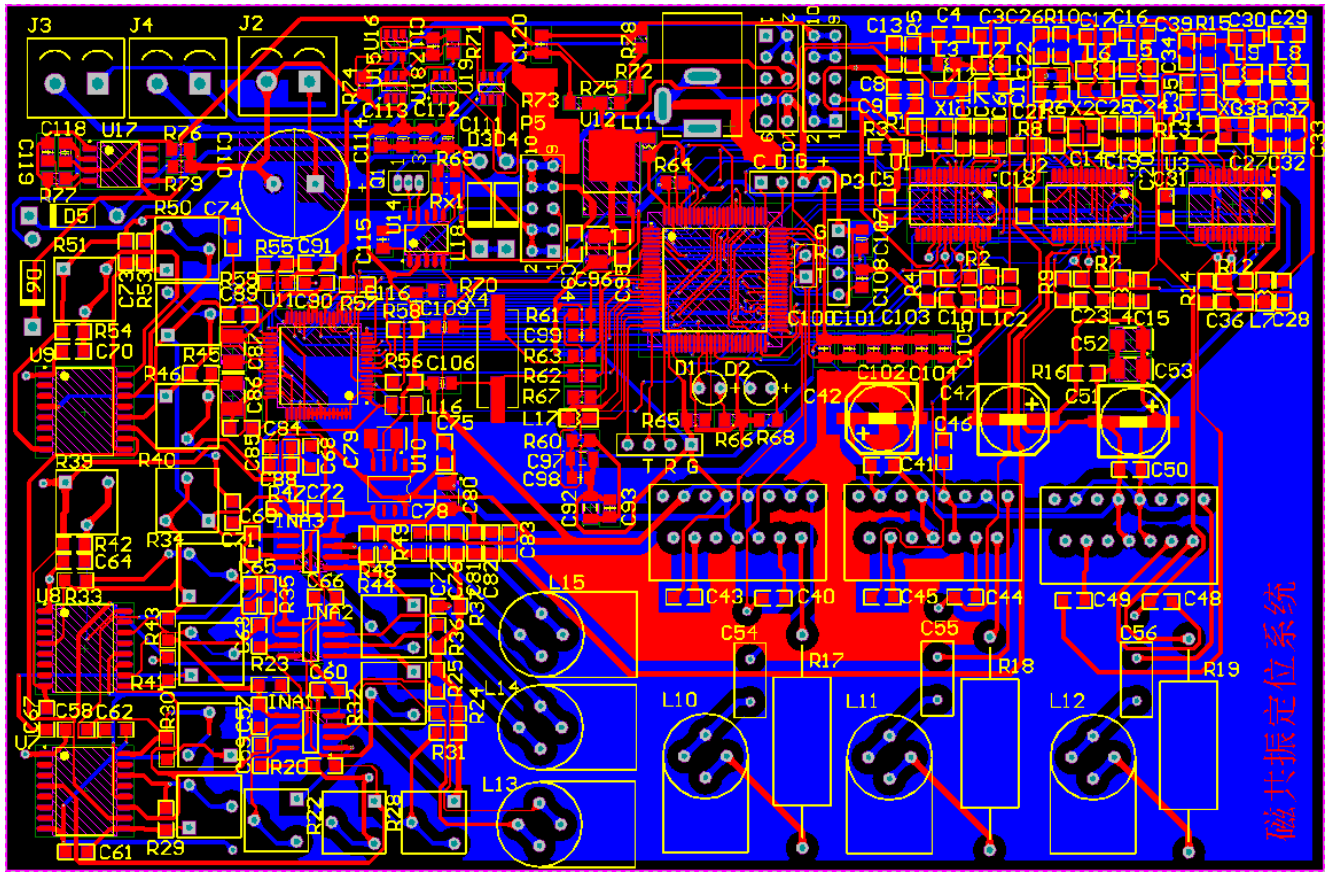

Fig. 28. The PCB diagram of hardware circuit.

program, the STM32 external chip driver and the magnetic positioning of the lower computer program.

The driver for the analog to digital conversion chip is shown as Fig. 30. It mainly includes the enumeration definition of the chip analog voltage input range and the number of acquisition and filtering times, the first-in-first-out queue definition of the ad conversion voltage storage structure, the initialization, the configuration, the setting filter, the scan, the start conversion and the read voltage function.

The driver for the DDS chip is shown as Fig. 31. It mainly includes the index number and frequency variable definition of the generated signal, as well as the definition of three DDS chips, initialization program, reset program, and configuration program.

```
#define MAX_AD_REAL     5.0

typedef enum
{
    AD7606InputRange_5V = 0,
    AD7606InputRange_10V = 1,
}AD7606InputRange_e;

typedef enum
{
    AD7606OS_No = 0,
    AD7606OS_2 = 1,
    AD7606OS_4 = 2,
    AD7606OS_8 = 3,
    AD7606OS_16 = 4,
    AD7606OS_32 = 5,
    AD7606OS_64 = 6,
}AD7606OS_e;

typedef struct
{
    bool IsFull;
    uint16_t Rear;
    int16_t Buffer[FIFO_SIZE];
}Fifo_t;

extern int16_t ADC_Convert[CHANNAL_NUM];
extern Fifo_t ADC_Fifo[AD_NUM];

void Fifo_AddData(Fifo_t *This , int16_t data);

void AD7606_ConfigAll(void);
int16_t AD7606_ReadParrelData(void);
void AD7606_SetOS(AD7606OS_e os);
void AD7606_Reset(void);
bool AD7606_IsBusy();
void AD7606_Scan(void);
void AD7606_StartConversion(void);
void AD7606_SetInputRange(AD7606InputRange_e inputRange);
int16_t AD7606_ReadAdc(unsigned char channel);
double AD7606_ReadAdcReal(unsigned char channel);
```

Fig. 30. The driver for the analog to digital conversion chip.

Because the serial port sending program and receiving program need to use the queue data structure. The STM32 queue program is shown as Fig. 32. It mainly includes the definition of queue, the definition of queue storage type, clear queue

```
#ifndef __USER_AD9850_H_
#define __USER_AD9850_H_

#include <Arduino.h>

#include "stdint.h"
#include "stdbool.h"
#include "mylib.h"

#define AD9850_NUM 3

#define L1_FREQ 13500
#define L2_FREQ 15000
#define L3_FREQ 17500

#define AD9850_FREQ 110;

typedef struct
{
    unsigned char Number;
    double Frequence;
}DDS_t;

extern DDS_t AD9850[3];

void AD9850_CommomHardWareInit(void);
void AD9850_ResetWithParrel(DDS_t* dds);
void AD9850_WriteWithParrel(DDS_t* dds,unsigned char w0);

void AD9850_AllInit(void);
```

Fig. 31. The driver for the DDS chip.

function, initialize queue function, whether queue is empty function, queue peek function, get queue number function, get queue space function, get queue header element, enqueue function , dequeue function, traverse the queue function.

The engineering structure of the PC program is shown as Fig. 33, which is mainly a software 3D model display window. The main function of the host computer is to perform positioning solution and 3D model display. The program is mainly shown in Fig. 34 and Fig. 35.

```
extern Queue* Queue_Byte;

#ifdef HaveBool

#include <stdbool.h>

bool CreateQueue(Queue *pQueue,unsigned int size);
bool InitQueue(Queue *pQueue);
bool IsEmpty(Queue *pQueue);
bool Peek(Queue *pQueue,QueueType *pe);

#else

#define BOOL int
#define TRUE 1
#define FALSE 0

BOOL CreateQueue(Queue *pQueue,unsigned int size);
BOOL InitQueue(Queue *pQueue);
BOOL IsEmpty(Queue *pQueue);
BOOL Peek(Queue *pQueue,QueueType *pe);

#endif

void ClearQueue( Queue *pQueue );
unsigned int GetCount( Queue *pQueue );
unsigned int GetSize(Queue *pQueue);
int IndexOf(Queue *pQueue,QueueType value);
QueueType ValueAt(Queue *pQueue,unsigned int index);
int GetHead(Queue *pQueue);
int EnQueue(Queue *pQueue , QueueType value);
int DeQueue( Queue *pQueue, QueueType *pe );
QueueType GetInQueue(Queue *pQueue);
void Queue_ForEach( Queue *pQueue, void (*func)(QueueType *pe) );
```

Fig. 32. The STM32 queue program.

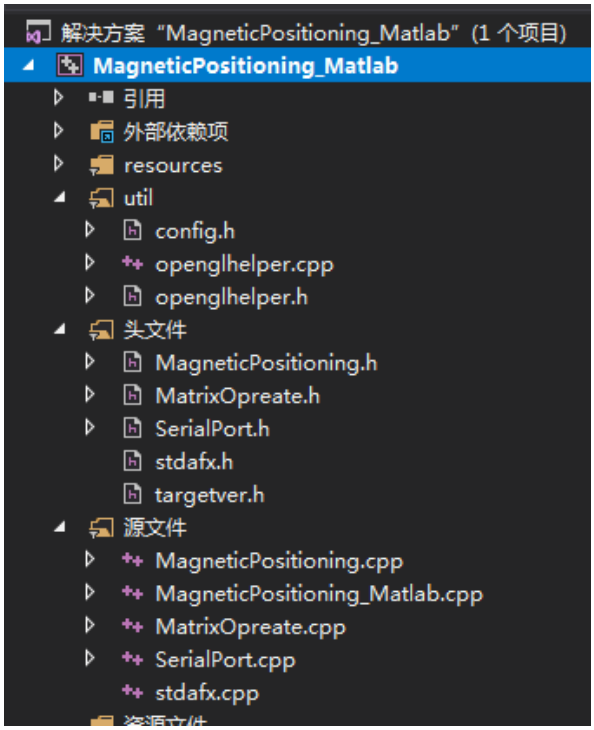

Fig. 33. The engineering structure of the PC program.

```
int flag = 0;
double  x_pre, y_pre, z_pre;
double distance1, distance2;
double xfinal, yfinal, zfinal;
double Xx; double Yx; double Zx;
double Xy; double Yy; double Zy;
double Xz; double Yz; double Zz;

double Px, Py, Pz, sumpxpypz;


Xx = F4_matrix[0][0]; Yx = F4_matrix[0][1]; Zx = F4_matrix[0][2];
Xy = F4_matrix[1][0]; Yy = F4_matrix[1][1]; Zy = F4_matrix[1][2];
Xz = F4_matrix[2][0]; Yz = F4_matrix[2][1]; Zz = F4_matrix[2][2];

Px = SumSquare(Xx, Xy, Xz);
Py = SumSquare(Yx, Yy, Yz);
Pz = SumSquare(Zx, Zy, Zz);
sumpxpypz = Px + Py + Pz;
PxPyPz[0][0] = Px; PxPyPz[1][0] = Py; PxPyPz[2][0] = Pz;
// 计算距离
rho = 1.5*constant*constant / sumpxpypz;
rho = pow(rho, 0.166667);

//求矩阵A1
for (int i = 0; i < 3; i++) {
    A1_matrix[i][0] = 0.0;
    for (int j = 0; j < 3; j++) {
        A1_matrix[i][0] = A1_matrix[i][0] + constant_matrix[i][j] *
    }
}
for (int i = 0; i < 3; i++)
```

Fig. 34. The positioning solution program.

```
void DrawSolidBoxWithColor(float a, float b, float c,
    float red = CUBE_COLOR_R,
    float blue = CUBE_COLOR_B,
    float green = CUBE_COLOR_B)
{
    auto object = gluNewQuadric();
    gluQuadricNormals(object, GLU_SMOOTH);
    gluQuadricTexture(object, GL_TRUE);
    glPushMatrix();
    //画第一个面
    glColor3f(red, blue, green);
    glRectf(0, 0, a, b);
    //画第二个面
    glRotatef(-90, 0, 1, 0);
    glRectf(0, 0, c, b);
    glRotatef(90, 0, 1, 0);
    //画第三个面
    glRotatef(90, 1, 0, 0);
    glRectf(0, 0, a, c);
    glRotatef(-90, 1, 0, 0);
    //画第四个面
    glTranslatef(0, 0, c);
    glRectf(0, 0, a, b);
    //画第五个面
    glTranslatef(a, b, -c);
    glRotatef(180, 0, 0, 1);
    glRotatef(-90, 0, 1, 0);
    glRectf(0, 0, c, b);
    glRotatef(90, 0, 1, 0);
    //画第六个面
    glRotatef(90, 1, 0, 0);
    glRectf(0, 0, a, c);
    glRotatef(-90, 1, 0, 0);
    //绘图回到原点
    glRotatef(-180, 0, 0, 1);
```

Fig. 35. The 3D model display program.

基于步进频信号磁共振原理的定位与能量传输一体化系统研究

学术诚信声明承诺书

本参赛团队声明所提交的论文是在指导老师指导下进行的研究工作和取得的研究成果。尽本团队所知，除了文中特别加以标注和致谢中所罗列的内容以外，论文中不包含其他人已经发表或撰写过的研究成果。若有不实之处，本人愿意承担一切相关责任。

参赛队员：刘昱麟　　指导老师：**Jim Harris**

Acknowledgement

I sincerely thank the organizers and sponsors of this competition, and express my gratitude to all those who helped me during the writing of this thesis.

My deepest gratitude goes first and foremost to my teacher and my supervisor, for their constant encouragement and guidance. They have walked me through all the stages of the writing of this thesis. Without their consistent and illuminating instruction, this thesis could not have reached its present form. They helped me design the experiments and build the chirp signal.

Last, my thanks would go to my beloved family for their loving considerations and great confidence in me. I also owe my sincere gratitude to my friends who gave me their help during the difficult course of the thesis.